

VE-Mobicast: A Variant-Egg-Based Mobicast Routing Protocol for Sensornets

Yuh-Shyan Chen and Shin-Yi Ann

Department of Computer Science and Information Engineering

National Chung Cheng University

Chiayi, Taiwan, 621, R.O.C.

E-mail: yschen@cs.ccu.edu.tw

Abstract—In this paper, we present a new "spatiotemporal multicast" protocol for supporting applications which require spatiotemporal coordination in sensornets. Existing mobicast routing protocols estimate and predict the forwarding zone without considering the factor of the moving direction; therefore a low predicted accuracy of the forwarding zone exists if the mobicast routing protocols additionally consider the factor of the moving direction. To simultaneously consider the factors of moving speed and direction, this work mainly investigates a new mobicast routing protocol, called variant-egg-based mobicast (VE-mobicast) routing protocol, by utilizing the variant-egg shape of the forwarding zone to achieve a high predicted accuracy. The contributions of our VE-mobicast routing protocol are summarized as follows: (1) our VE-mobicast protocol builds a new shape of a forwarding zone, called the variant-egg, to adaptively and efficiently determine the location and shape of the forwarding zone to maintain the same number of wake-up sensor nodes; (2) our VE-mobicast protocol is a fully distributed algorithm which reduces the communication overhead of determining the forwarding zone and the mobicast message forwarding overhead; (3) our VE-mobicast routing protocol can improve the predicted accuracy of the forwarding zone by considering the factors of moving speed and direction. Finally, the simulation results illustrate the performance achievements, compared to existing mobicast routing protocols.

Index Terms: Sensornet, wireless communication, mobile computing, mobicast, routing, distribution.

I. INTRODUCTION

Sensornets [1] are large-scale distributed embedded systems composed of a large number of small-sized, low-cost, and low-power devices that integrate sensors, actuators, wireless communication, and microprocessors. In sensornets, sensor nodes are always set up in hazardous or faraway environments due to their disposable capability. The limited energy is a scarce resource in sensornets, and so it has to be wisely managed to extend the sensornet lifetime. This work focuses on developing power-aware routing protocols to support many variable sensornet applications. Existing power-aware routing schemes are investigated [6].

Recently, a new "spatiotemporal multicast" was presented for supporting applications which require spatiotemporal coordination in sensornets. Existing protocols for a spatiotemporal variant of a multicast called a "mobicast" were designed to support a forwarding zone that moves at a constant velocity, \vec{v} , in the sensornet. The spatiotemporal character of the

mobicast is to forward a mobicast message to all nodes that will be present at time t in some geographic zone (called a forwarding zone), F , where both the location and shape of the forwarding zone are a function of time over some interval (t_{start}, t_{end}) . The mobicast is constructed by a series of forwarding zones over different intervals (t_{start}, t_{end}) , and sensor nodes located in the forwarding zone at the time interval (t_{start}, t_{end}) should wake up in order to save power. Huang *et al.* recently developed three mobicast routing protocols [7][8][9]. First, Huang *et al.* [8] initially designed a spatiotemporal multicast protocol for sensornets. Huang *et al.* [7] then presented a new energy-efficient spatiotemporal multicast protocol for sensornets. More recently, Huang *et al.* [9] proposed a reliable mobicast protocol via face-aware routing (FAR) in sensornets. There are many useful applications using mobicast routing protocols, such as object tracking [2] and environmental monitoring [5]. The face-aware approach is originated by Bose *et al.* [4]. They consider the routing problems in ad hoc wireless networks modeled as *unit graphs* (faces) in which nodes are points in the plane and two nodes can communicate if the distance between them is less than some fixed unit. Bose and Morin [3] describe an algorithm for enumerating all the faces, edges, and vertices of a connected embedded planar graph G without the use of mark bits or a stack. Existing mobicast routing protocols [7][8][9] estimate and predict the forwarding zone without considering the factor of moving direction; therefore a low predicted accuracy of the forwarding zone exists if existing mobicast routing protocols additionally consider the factor of the moving direction.

The rest of this paper is organized as follows. Section II presents the basic ideas and challenges of our routing protocol. Our proposed VE-mobicast protocol is presented in section III. Section IV gives the performance analysis. Finally, section V concludes this paper.

II. BASIC IDEAS AND CHALLENGES

This section introduces a new special case of a "spatiotemporal multicast" protocol for supporting applications which require spatiotemporal coordination in sensornets. This spatiotemporal multicast protocol provides sensing applications that need to disseminate the multicast message to the "right" place (or prescribed zone) at the "right" time. A spatiotemporal multicast session is specified by $\langle m, Z[t], T_s, T \rangle$, which is

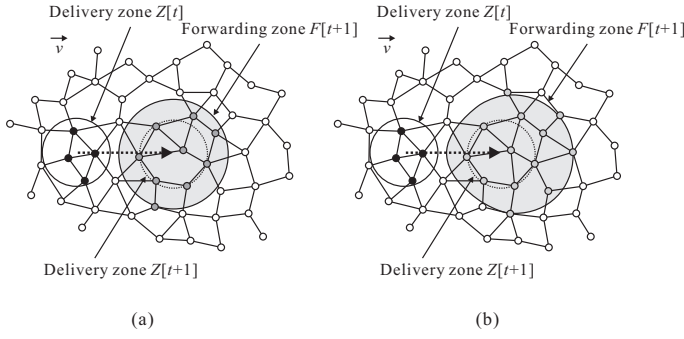


Fig. 1. Spatiotemporal multicast and VE-mobicast.

formally defined in [8], where m is the multicast message, $Z[t]$ describes the expected area of message delivery at time t , and T_s and T are the sending time and duration of the multicast session, respectively. As the delivery zone $Z[t]$ evolves over time, the set of recipients for m changes as well.

A special case of a spatiotemporal multicast, called a mobicast, was considered in [7][8][9]. The delivery zone is some fixed convex polygon, P , that translates through 2-D space at some constant velocity, \vec{v} [8]; i.e., $Z[t] = P[\vec{r}_0 + \vec{v}(t - T_s)]$ with $P[\vec{r}_0]$ being the polygon centered at \vec{r}_0 . Huang *et al.* call this special class of spatiotemporal multicasts a "constant velocity mobicast" or "mobicast" [7][8][9]. Observe that, the polygonal shape of the delivery zone adopted a circular shape in those works [7][8][9]. Figure 1(a) shows an example of the delivery zones $Z[t]$ and $Z[t+1]$.

In general, the mobicast routing protocol is composed of a delivery zone and a forwarding zone. The forwarding zone [8] is defined as every sensor node in forwarding zone $F[t+1]$ being responsible for forwarding the mobicast messages to guarantee that delivery zone $Z[t+1]$ at time $t+1$ can successfully receive the mobicast message. The size of forwarding zone $F[t+1]$ is always larger than the size of delivery zone $Z[t+1]$. An example of a forwarding zone is given in Fig. 1(a). The key problem of the mobicast protocol is how to predict and estimate the correct size and shape of forwarding zone $F[t+1]$ at time t . Efforts are made in this work to develop a fully distributed algorithm to increase the reliability and decrease the communication overhead. In our proposed variant-egg-based scheme, the shape of forwarding zone $F[i]$ at time i is a variant egg, which is denoted as F_{VE} or $F_{VE}[i]$ in this work, where $0 \leq i$, as illustrated in Fig. 1(b).

III. VE-MOBICAST: VARIANT-EGG-BASED MOBICAST ROUTING PROTOCOL

In our VE-mobicast approach, hold-and-forward zone $H[t] = F_{VE}[t] \cap F_{VE}[t+1]$. An example of hold-and-forward zone $H[t]$ is given in Fig. 2.

- (1) Egg estimation phase: The size of the variant-egg forwarding zone, $F_{VE}[t+1]$, at time t is estimated by sensor nodes in $H[t]$. The forwarding zone [7][8][9] limits retransmission to a bounded space while ensuring

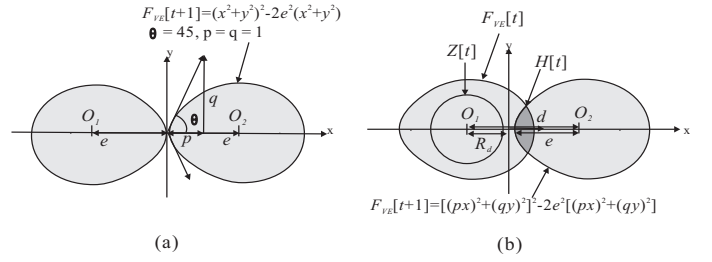


Fig. 2. Equations of (a) the VE-mobicast and (b) the Cassini Oval.

that all sensor nodes that need to receive the mobicast message do so.

- (2) Distributed variant-egg-based mobicast phase: With the estimated $F_{VE}[t+1]$, a distributed algorithm of VE-mobicast operation is presented for all sensor nodes in $H[t]$. This operation can dynamically adjust the shape of the variant-egg forwarding zone, $F_{VE}[t+1]$, at time t .

The detailed operations of the variant-egg estimation and distributed VE-mobicast phases are described as follows.

A. Phase I: Egg Estimation

All sensor nodes in $H[t]$ estimate the shape and size of variant-egg $F_{VE}[t+1]$ at time t for the incoming forwarding zone, $Z[t+1]$. The shape of the variant-egg is calculated from the Cassini Oval equation [10]. Based on Cassini Oval equation [10], the equation of our variant-egg forwarding zone is,

$$[(px)^2 + (qy)^2]^2 - 2e^2[(px)^2 + (qy)^2] = 0,$$

$$\text{where } \tan \theta = \frac{q}{p} \text{ and } p \times q = 1.$$

Observe that the forwarding zone can dynamically change shape by changing the ratio of x and y if the egg area is fixed, and px is p multiples of x and qy is q multiple of y , where $p \times q = 1$. For instance with a fixed egg area, $p = q = 1$, or $p = 3$ and $q = \frac{1}{3}$. More specifically, if the area of our variant-egg forwarding zone, $F_{VE}[t+1]$, is e^2 , $\theta = 45^\circ$, $p = q = 1$, and $e = \pi^{\frac{1}{2}} R_d$, then the equation becomes

$$(x^2 + y^2)^2 - 2e^2(x^2 + y^2) = 0.$$

Fig. 2(a) shows an example of $F_{VE}[t+1]$ where O_1 and O_2 denote two fixed points, O_2 is the center of the variant-egg forwarding zones, and $2e$ is the distance between the fixed points of O_1 and O_2 . In the following, our VE-mobicast routing protocol adopts the half portion of the lemniscate as our variant-egg forwarding zone $F_{VE}[t+1]$. An example is shown in Fig. 2(b).

One important aspect is deciding whether or not sensor node (a, b) is located in variant-egg forwarding zone $F_{VE}[t+1]$. If $(x^2 + y^2)^2 - 2e^2(x^2 + y^2) = (a^2 + b^2)^2 - 2e^2(a^2 + b^2) \leq 0$, then (a, b) is located in variant-egg forwarding zone $F_{VE}[t+1]$. If $(x^2 + y^2)^2 - 2e^2(x^2 + y^2) = (a^2 + b^2)^2 - 2e^2(a^2 + b^2) > 0$, then (a, b) is out of variant-egg forwarding zone $F_{VE}[t+1]$. Fig.

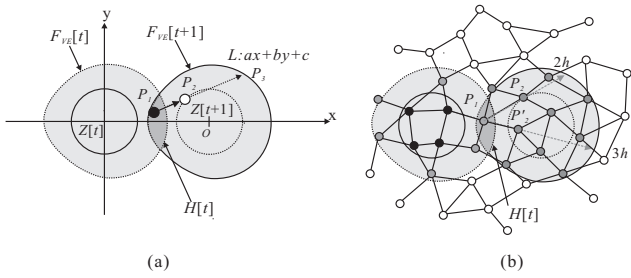


Fig. 3. Estimation phase of a VE-mobicast.

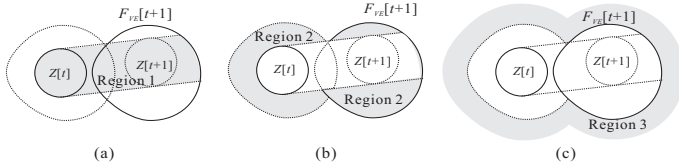


Fig. 4. Three different regions.

3(a) shows an example of this. The egg estimation algorithm is given.

- S1:** The first task is to decide whether or not sensor node P_1 at (a_1, b_1) is located in hold-and-forward zone $H[t] = F_{VE}[t] \cap F_{VE}[t+1]$. Sensor node P_1 is within $H[t]$ if P_1 is within $F_{VE}[t]$ and P_1 is also within $F_{VE}[t+1]$; that is, $(x^2 + y^2)^2 - 2e^2(x^2 + y^2) = (a_1^2 + b_1^2)^2 - 2e^2(a_1^2 + b_1^2) \leq 0$.
- S2:** Let sensor node P_1 at (a_1, b_1) be within hold-and-forward zone $H[t]$ and sensor node P_2 at (a_2, b_2) be within $F_{VE}[t+1]$, and P_1 and P_2 are a pair of neighboring nodes. A hop count is needed to estimate the hop-distance from P_1 through P_2 to the boundary of $F_{VE}[t+1]$. This hop count is very useful in phase II to provide a distributed algorithm of the variant-egg-based mobicast. Let the line equation of P_1 and P_2 be $ax + by + c = 0$ and the equation of $F_{VE}[t+1]$ be $(x^2 + y^2)^2 - 2e^2(x^2 + y^2)$. Let P_3 be the intersection point of the line and $F_{VE}[t+1]$; that is, $ax + by + c = (x^2 + y^2)^2 - 2e^2(x^2 + y^2)$. Then, $\overline{P_2P_3}$ is the distance between P_2 and P_3 . Sensor node P_1 , in anticipation, forwards a mobicast message through P_2 within $\frac{\overline{P_2P_3}}{r} + 1$ hops, where r is the communication radius of the sensor node. An example is illustrated in Fig. 3(b), where the estimated hop counts from P_1 through P_2 and P_2' are two and three, respectively.

B. Phase II: Distributed Variant-Egg-Based Mobicast

A simple control packet, denoted $P_{VE}(p, q, \frac{h}{H}, N_{11}N_{12} \dots N_{1i})_{t_x}$, is adopted in this work for developing the distributed algorithm, where p and q are used to dynamically change the shape of the forwarding zone, $\frac{h}{H}$ is used to limit the number of packets forwarded, $N_{11}N_{12} \dots N_{1i}$ maintain the path history, and packet P_{VE} is forwarded at time t_x .

Assume that all sensor nodes are uniformly distributed in an area. This area is divided into three kind of regions. Without loss of generality, we only consider the case of a pair of

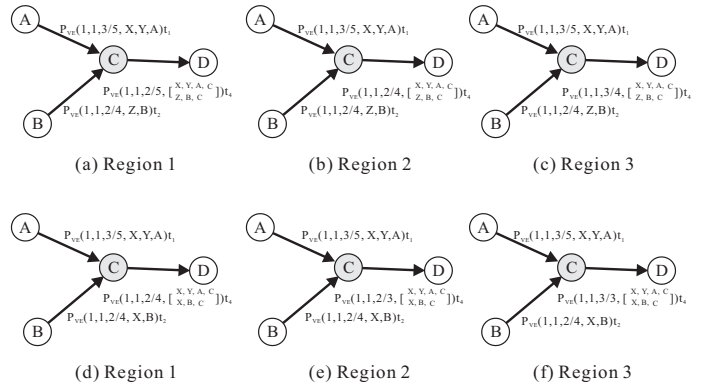


Fig. 5. Examples of merging operations.

adjacent delivery zones, $Z[t]$ and $Z[t+1]$, and a pair of forwarding zones, $F_{VE}[t]$ and $F_{VE}[t+1]$, to explain the three regions as follows.

- Region 1: A path moves from $Z[t]$ to $Z[t+1]$, as illustrated in Fig. 4(a).
- Region 2: $F_{VE}[t] \cup F_{VE}[t+1] - \text{Region 1}$, as illustrated in Fig. 4(b).
- Region 3: $\sim(F_{VE}[t] \cup F_{VE}[t+1])$, as illustrated in Fig. 4(c).

The distributed algorithm of the VE-mobicast operation is given here.

- S1:** A sensor node, P_i , is in $H[t]$ and P_j is in $F_{VE}[t+1]$, where P_i and P_j are neighboring nodes. Sensor node P_i initiates and floods a $P_{VE}(p, q, \frac{1}{H}, P_i)_{t_x}$ packet to neighboring sensor node P_j at time $t_x = t_1$, where H is the hop count calculated in phase I.
- S2:** Sensor node P_i receives $P_{VE}(p, q, \frac{h_1}{H_1}, N_{1,1}N_{1,2} \dots N_{1,i-1})_{t'_{x_1}}$, the first packet from $N_{1,i-1}$, at time t'_{x_1} . The sensor node waits a period of time, t'_y , for receiving additional different P_{VE} packets, where $t'_y = t'_{x_1} + d + \text{backoff_time}$ and d is the degree of P_i . Assuming that $P_{VE}(p, q, \frac{h_1}{H_1}, N_{1,1}N_{1,2} \dots N_{1,i-1})_{t'_{x_1}}$, $P_{VE}(p, q, \frac{h_2}{H_2}, N_{2,1}N_{2,2} \dots N_{2,i-1})_{t'_{x_2}}, \dots$, and $P_{VE}(p, q, \frac{h_m}{H_m}, N_{m,1}N_{m,2} \dots N_{m,i-1})_{t'_{x_m}}$ packets are received at node P before time t'_y , then m P_{VE} packets are merged into one P_{VE} packet, denoted

$$P_{VE}(p, q, \frac{h_{\text{merge}}}{H_{\text{merge}}}, \left[\begin{array}{c} N_{1,1}N_{1,2} \dots N_{1,i-1}, P_i \\ \vdots \\ N_{m,1}N_{m,2} \dots N_{m,i-1}, P_i \end{array} \right]_{t'_y}).$$

The merging operation, which is dependent on the position of sensor node P_i , is given here.

1. Let $\frac{h_{\text{merge}}}{H_{\text{merge}}} = \frac{\text{Min } h_i}{\text{Max } H_i}$ if P_i is in region 1.
2. Let $\frac{h_{\text{merge}}}{H_{\text{merge}}} = \frac{\text{Min } h_i}{\text{Min } H_i}$ if P_i is in region 2.
3. Let $\frac{h_{\text{merge}}}{H_{\text{merge}}} = \frac{\text{Max } h_i}{\text{Min } H_i}$ if P_i is in region 3.

- S3:** If there are the same n predecessor nodes for all

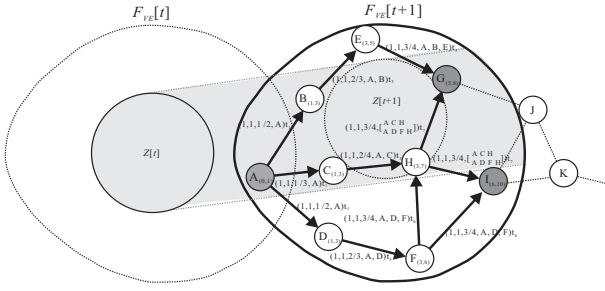


Fig. 6. Scenario of the no "hole" problem.

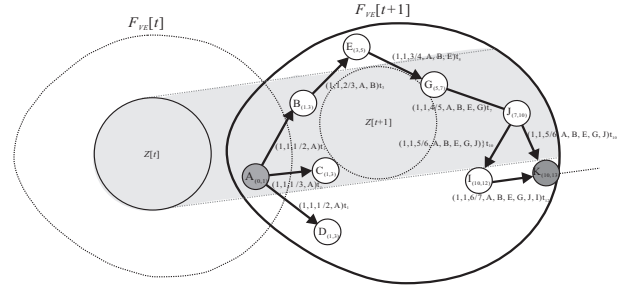


Fig. 7. Scenario of the "hole" problem.

path-histories of $\begin{bmatrix} N_{1,1}N_{1,2}\dots N_{1,i-1}, P_i \\ \vdots \\ N_{m,1}N_{m,2}\dots N_{m,i-1}, P_i \end{bmatrix}$, then let $H_{merge} = H_{merge} - n$. After that, the $P_{VE}(p, q, \frac{h_{merge}}{H_{merge}}, \begin{bmatrix} N_{1,1}N_{1,2}\dots N_{1,i-1}, P_i \\ \vdots \\ N_{m,1}N_{m,2}\dots N_{m,i-1}, P_i \end{bmatrix})_{t_y}$ packet is forwarded if $\frac{h_{merge}}{H_{merge}} < 1$ at time t'_y .

Examples of merging operations in step **S2** are given in Fig. 5(a), for $\theta = 45^\circ$ and $p = q = 1$. If sensor node C is in region 1, sensor node C receives $P_{VE}(1, 1, \frac{3}{5}, X, Y, A)_{t_1}$ and $P_{VE}(1, 1, \frac{2}{4}, Z, B)_{t_2}$, and the merged packet is $P_{VE}(1, 1, \frac{2}{5}, \begin{bmatrix} X, Y, A, C \\ Z, B, C \end{bmatrix})_{t_4}$ since the same predecessor sensor node does not exist. Fig. 5(d) gives an explanation if sensor node C is in region 1, sensor node C receives $P_{VE}(1, 1, \frac{3}{5}, X, Y, A)_{t_1}$ and $P_{VE}(1, 1, \frac{2}{4}, X, B)_{t_2}$, and the merged packet is $P_{VE}(1, 1, \frac{2}{4}, \begin{bmatrix} X, Y, A, C \\ X, B, C \end{bmatrix})_{t_4}$ because X is the same predecessor sensor node. As illustrated in Fig. 5(b), if sensor node C is in region 2 and sensor node C receives $P_{VE}(1, 1, \frac{3}{5}, X, Y, A)_{t_1}$ and $P_{VE}(1, 1, \frac{2}{4}, Z, B)_{t_2}$, then the merged packet is $P_{VE}(1, 1, \frac{2}{4}, \begin{bmatrix} X, Y, A, C \\ Z, B, C \end{bmatrix})_{t_4}$, since the same predecessor sensor node does not exist. Fig. 5(e) shows that if sensor node C is in region 2 and sensor node C receives $P_{VE}(1, 1, \frac{3}{5}, X, Y, A)_{t_1}$ and $P_{VE}(1, 1, \frac{2}{4}, X, B)_{t_2}$, then the merged packet is $P_{VE}(1, 1, \frac{2}{3}, \begin{bmatrix} X, Y, A, C \\ X, B, C \end{bmatrix})_{t_4}$, since X is the same predecessor sensor node. Finally, as shown in Fig. 5(c), if sensor node C is in region 3 and sensor node C receives $P_{VE}(1, 1, \frac{3}{5}, X, Y, A)_{t_1}$ and $P_{VE}(1, 1, \frac{2}{4}, Z, B)_{t_2}$, then the merged packet is $P_{VE}(1, 1, \frac{3}{4}, \begin{bmatrix} X, Y, A, C \\ Z, B, C \end{bmatrix})_{t_4}$, since the same predecessor sensor node does not exist. Fig. 5(f) shows that if sensor node C is in region 3, sensor node C receives $P_{VE}(1, 1, \frac{3}{5}, X, Y, A)_{t_1}$ and $P_{VE}(1, 1, \frac{2}{4}, X, B)_{t_2}$, then the merged packet is $P_{VE}(1, 1, \frac{3}{3}, \begin{bmatrix} X, Y, A, C \\ X, B, C \end{bmatrix})_{t_4}$, since X is the same predecessor sensor node.

In step **S3**, it was observed that $\frac{h_{merge}}{H_{merge}}$ is used to determine whether or not the P_{VE} packet should be forwarded, where h_{merge} denotes the hop number which the current P_{VE} packet

traverses and H_{merge} is the estimated hop count toward the boundary of $F_{VE}[t+1]$. If the ratio of $\frac{h_{merge}}{H_{merge}} < 1$, the P_{VE} packet should be forwarded since $h_{merge} < H_{merge}$. If the ratio of $\frac{h_{merge}}{H_{merge}} \geq 1$, the P_{VE} packet can be forwarded since $h_{merge} \geq H_{merge}$.

Finally, two scenarios are given in Fig. 6 and Fig. 7 to discuss the effect of the 'hole' problem. Fig. 7 has a 'hole' in the $F_{VE}[t+1]$, but Fig. 6 has no 'hole' in $F_{VE}[t+1]$. As illustrated in Fig. 6, since a merging operation is executed in node G , then the P_{VE} message sent from node A is stopped in node G . As shown in Fig. 7, there is no merging operation in node G , therefore the P_{VE} message sent from node A is stopped in node K .

IV. PERFORMANCE ANALYSIS

In the following, we use "VE-mobicast", "mobicast", and "FAR" to denote our protocol, Huang *et al.*'s mobicast protocol [8], and Huang *et al.*'s FAR protocol [9]. Before describing the performance metrics, the *rotation frequency* (RF) and *rotation angle* (RA) are defined. The RA is the rotation angle between two zones, $Z[t]$ and $Z[t+1]$, if a rotation occurs at times t and $t+1$. The RA ranges from 5° to 50° in the simulation. The RF is the rotation frequency of changing the rotation angle for a spatiotemporal application. The RF ranges from 10% to 100% in our simulation. The performance metrics of the simulation are given below.

- *Predicted accuracy* (PA): The percentage of sensor nodes located in both $Z[t+1]$ and $F[t+1]$ divided by the total number of sensor nodes in $F[t+1]$.

A. Effect of Rotation Frequency and Rotation Angle

When the network density is 10 nodes/ m^2 , Fig. 8 shows the simulation results of predicted accuracy (PA) under the effect of rotation frequency (RF) and rotation angle (RA). The high value of the PA implies that a high predicted accuracy was obtained to predict the direction of the spatiotemporal application with high accuracy. Figs. 8(a)(b)(c) show the performance of PA of the mobicast, FAR and VE-mobicast routing protocols. On average, the curve of the PA of the mobicast is lower than that of the FAR, and the curve of the PA of the FAR is lower than that of the VE-mobicast. Fig. 8(d) calculates the average PA results for the mobicast, FAR, and VE-mobicast. Observe that the average PA herein is calculated

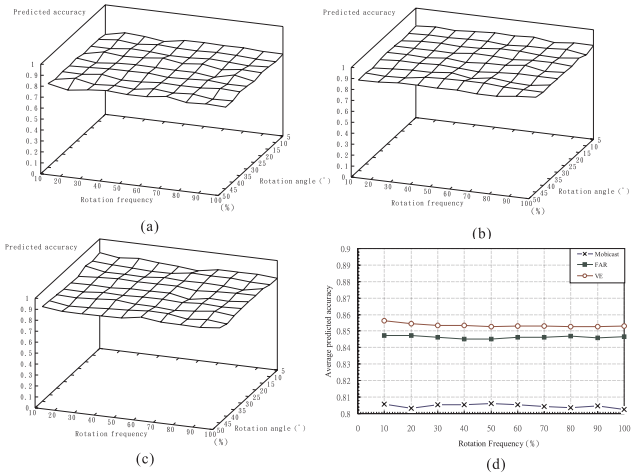


Fig. 8. Performance of the predicted accuracy vs. the rotation frequency and rotation angle.

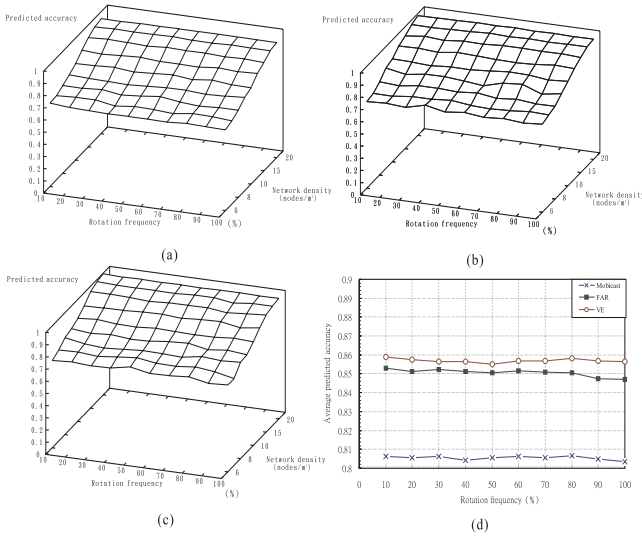


Fig. 9. Performance of the predicted accuracy vs. the rotation frequency and network density.

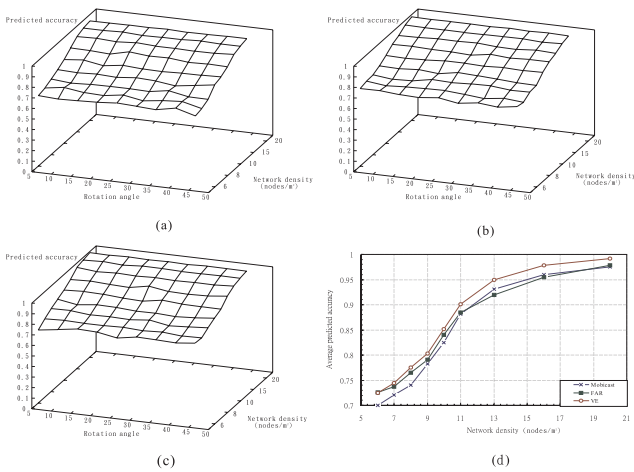


Fig. 10. Performance of the predicted accuracy vs. the network density and rotation angle.

by the average value of the PA for all possible rotation angles (ranging from 5° to 50°). We observed the results to be the average PA of mobicast $<$ that of FAR $<$ that of VE-mobicast.

B. Effect of Rotation Frequency and. Network Density

When the rotation angle is 15° , Fig. 9 shows the simulation results of PA under the effect of RF and network density (ND). Fig. 9(a)(b)(c) show that the higher the ND is, the higher the PA of the VE-mobicast will be. Similar results were obtained that the average PA of mobicast $<$ that of FAR $<$ that of VE-mobicast, where the average PA herein was calculated by taking the average value of the PAs for all possible NDs.

C. Effect of Network Density and Rotation Angle

When the RF is 50%, Fig. 10 shows the simulation results of PA under the effect of RF and RA. Fig. 10(a)(b)(c) show that the higher the ND is, the higher the PA of the VE-mobicast will be. Similar results were obtained that the average PA of mobicast $<$ that of FAR $<$ that of VE-mobicast, where the average PA herein was calculated by taking the average value of the PA for all possible NDs.

V. CONCLUSIONS

In this paper, we mainly investigated a new mobicast routing protocol, called variant-egg-based mobicast (VE-mobicast) routing protocol, by utilizing the variant-egg shape of the forwarding zone to achieve mobicast forwarding with a high predicted accuracy. The simulation results illustrated the performance achievements, compared to existing mobicast routing protocols.

REFERENCES

- [1] I. F. Akyildiz, W. Su, Y. Sankarasubramaniam, and E. Cayirci. "A Survey on Sensor Network". *IEEE communications Magazine*, 40:102–114, August 2002.
- [2] P. Bauer, M. Sichitiu, R. Istepanian, and K. Premaratne. "The Mobile Patient: Wireless Distributed Sensor Networks for Patient Monitoring and Care". *Proceedings of the IEEE Conference on Information Technology Applications in Biomedicine (ITAB)*, pages 17–21, November 2000.
- [3] P. Bose and P. Morin. "An Imporved Algorithm for Subdivision Traversal without Extra Storage". *International Journal of Foundations of Computer Science*, pages 297–308, 2002.
- [4] P. Bose, P. Morin, I. Stojmenovic, and J. Urrutia. "Routing with Guaranteed Delivery in Ad Hoc Wireless Networks". *ACM Wireless Networks*, 3(4):609–616, 2001.
- [5] A. Cerpa, J. Elson, D. Estrin, L. Girod, M. Hamilton, and J. Zhao. "Habitat Monitoring: Application Driver for Wireless Communications Technology". *Proceedings of IEEE Special Interest Group on Data Communication (SIGCOMM)*, pages 20–41, April 2001.
- [6] J. L. Gao. "An Adaptive Network/ Routing Algorithm for Energy Efficient Cooperative Signal Processing in Sensor Networks". *Proceedings of the IEEE Aerospace Conference*, 3:1117–1124, March 2002.
- [7] Q. Huang, C. Lu, and G.-C. Roman. "Spatiotemporal Multicast in Sensor Networks". *Proceedings of the ACM Conference on Embedded Networked Sensor Systems (SenSys)*, pages 205–217, November 2003.
- [8] Q. Huang, C. Lu, and G.-C. Roman. "Design and Analysis of Spatiotemporal Multicast Protocols for Wireless Sensor Networks". *Telecommunication Systems. Special Issue on Wireless Sensor Networks*, 26(2-4):129–160, August 2004.
- [9] Q. Huang, C. Lu, and G.-C. Roman. "Reliable Mobicast via Face-Aware Routing". *Proceedings of the IEEE International Conference on Computer Communications (INFOCOM)*, March 2004.
- [10] Eric W. Weisstein. Cassini ovals. *From MathWorld. A Wolfram Web Resource*. <http://mathworld.wolfram.com/CassiniOvals.html>.